Microfluid Nanofluid (2010) 8:275–282
DOI 10.1007/s10404-009-0516-4

SHORT COMMUNICATION

Capillary flow in microchannels

Y. Zhu · K. Petkovic-Duran

Received: 3 July 2009 / Accepted: 28 September 2009 / Published online: 19 November 2009

Abstract The surface of microchannels, especially polymer channels, often needs to be treated to acquire specific properties. This study investigated the capillary flow and the interface behavior in several glass capillaries and fabricated microchannels using a photographic technique and image analysis. The effect of air plasma treatment on the characteristics of capillary flow in three types of microfluidic chips, and the longevity of the acquired surface properties were also studied. It was observed that the dynamic contact angles in microchannels were significantly larger than those measured from a flat substrate and the angle varied with channel size. This suggests that dynamic contact angle measured in situ must be used in the theoretical calculation of capillary flow speed, especially for microfabricated microchannels since the surface properties are likely to be different from the native material. This study also revealed that plasma treatment could induce different interface patterns in the PDMS channels from those in the glass and PC channels. The PDMS channel walls could acquire different level of hydrophilicity during the plasma treatment, and the recovery to hydrophobicity is also non-homogeneous.

Keywords Microfluidic chip · Capillary flow · Plasma treatment

Y. Zhu (✉) · K. Petkovic-Duran
CSIRO Microfluidics Laboratory, CSIRO Division of Materials Science and Engineering, 37 Graham Road, P.O. Box 56, Highett, Melbourne, VIC 3190, Australia
e-mail: yonggang.zhu@csiro.au

K. Petkovic-Duran
e-mail: karolina.petkovicduran@csiro.au

1 Introduction

Microfluidics is one of the emerging science and technology areas. It refers to microfabricated fluidic systems that can process or manipulate small amount of fluids, typically of the order of nanoliters or smaller, using channels with geometries of length of microns to sub-millimeters. Microfluidics has attracted ever-increasing attention since its introduction in the early 1990s due to its advantages over conventional technologies such as reduced reagent consumption, fast reaction rate, short analysis time, and amenability to automation and mass production (Whitesides 2006). Microfluidic technologies are attracting interest in many fields, including chemistry, biology, medicine, sensing, and materials (e.g., Beebe et al. 2002; Squires and Quake 2005).

In the early stage of development, the microfluidic chips were mostly fabricated from silicon or glass materials due to the established fabrication methods by the semiconductor industry. Since the late-1990s, overwhelming effort has been devoted to developing polymer-based chips. This is mainly driven by the faster speed and lower cost in fabrication and the need for disposable chips for diagnostics and field-deployable devices. However, the surface of the polymers often needs to be treated (e.g., surface coating, plasma treatment etc.) to acquire specific properties to enable, e.g., surface charges required for electro-osmosis, wetting of the surfaces, and passive pumping of liquids. The quality and longevity of the surface treatment are important to maintain the functionality of the microfluidic chip.

There have been extensive investigations on the techniques for surface modification and characterization of the surface properties (see, for example, Fritz and Owen 1995; Kim et al. 2001; Lim et al. 2001; Belder and Ludwig 2003 for a review on pre-2003 work; Kirby et al. 2004; Martin et al. 2007; Klages et al. 2007; Bodas et al. 2008; Vourdas

et al. 2008; Moon and Vaziri 2009). Most of the previous studies reported the effect of surface modifications on the polymer properties such as zeta potential, hydrophobicity, contact angle, adhesion, and so on. Many of the studied polymer samples mostly appeared as flat and smooth substrates. These are very different from the inner wall surface of microchannels, which are typically formed by laser micromachining, injection molding, or hot-embossing.

Since 1990s, there have been a number of studies on capillary flows in microfabricated channels. For example, Kim et al. (1995) and Kim and Whitesides (1997) studied the imbibition and flow of wetting fluids in rectangular PDMS channels with self-assembled monolayers (SAMs) for controlling the hydrophilicity of the channel surfaces. Zhao et al. (2001) reported selective control of surfaces by forming a UV photocleavable SAM on glass surfaces to direct liquid flow inside microchannels. Capillary flow controls have been investigated for processing liquid samples (e.g., Junker et al. 2002; Chung et al. 2007). Lin and Burns (2005) investigated the capillary flow in several microchannels made from UV-treated COC, glass, and oxygen plasma-treated PDMS. Significant decay of flow speed was observed for the treated PDMS channel, but not reported data on treated COC chips. Lim et al. (2006) developed a polymer device with surfactant-containing adhesive film as capping layer to control the hydrophilicity. Jeong et al. (2007) studied capillary flow in poly(ethylene glycol) (PEG) and PDMS/glass hybrid microchannels. It was observed that the air–water interface in the PDMS/glass microchannel was of convex shape, which was opposite to the concave shape of the interface in the PEG microchannel. However, the measured capillary speed in PDMS microchannel departed significantly from the theoretical value. Chung et al. (2009) reported that the contact angle of PMMA could be significantly reduced within several hours of plasma treatment and restored to the initial value in about 6 months. They developed a technique by adding nanointerstices adjacent to microchannel to promote capillary flow.

Most of the studies discussed above measured the location of the interface as a function of time. Data are scarcely available on the interface shape and contact angle, especially after surface treatment (e.g., Lin and Burns 2005). Although Jeong et al. (2007) observed the convex air–water interface in the hybrid PDMS/glass microchannel, which was opposite to the concave shape of the interface in the PEG microchannel, the measured capillary speed in PDMS microchannel departed significantly from the theoretical value. This difference throws doubts on the choice of contact angle for the calculation since the contact angles on the channel wall surfaces may be significantly different from those of a smooth and flat surfaces. The aim of this study is to experimentally quantify the capillary flow rate for several commonly used substrates (glass, PC, and PDMS) and measure the contact angles for comparison with existing values reported on flat surfaces. The above measurements would provide useful information for calculating capillary flow in microchannels made from these materials. The second aim of the study is to examine the longevity of the capillary action of PDMS and PC chips and the interface change during the course of hydrophobic recovery.

2 Theoretical background

Consider a laminar horizontal flow through a straight circular channel of length L and a radius r (Fig. 1). The mean flow velocity u through the channel is given by (Landau and Lifshitz 1987)

$$u = -\frac{r^2}{8\mu}\frac{\Delta P}{L} \tag{1}$$

where ΔP is the total pressure drop along the channel, and μ is the fluid viscosity. In the general case of two immiscible fluids, Eq. 1 can be rewritten as

$$u = -a_0\frac{r^2}{8\mu_{\text{eff}}}\frac{\Delta P - P_c}{L}, \tag{2}$$

where $\mu_{\text{eff}} = \frac{x}{L}\mu_w + \frac{L-x}{L}\mu_a$ is the effective viscosity; μ_w and μ_a are viscosities for phase 1 and phase 2 fluids, respectively; x is the location of the interface measured from the inlet, P_c is the capillary pressure across the interface, and a_0 is a constant associated with the channel cross section shape. For a rectangular cross section with a height of h and width of w, the channel shape factor a_0 is given by (Brody et al. 1996; Ichikawa et al. 2004)

$$a_0 = \frac{64}{\pi^4}\sum_{n=0}^{\infty}\frac{1}{(2n+1)^4}\left\{1 - \frac{2h}{(2n+1)\pi w}\tanh\frac{(2n+1)\pi w}{2h}\right\}, \tag{3}$$

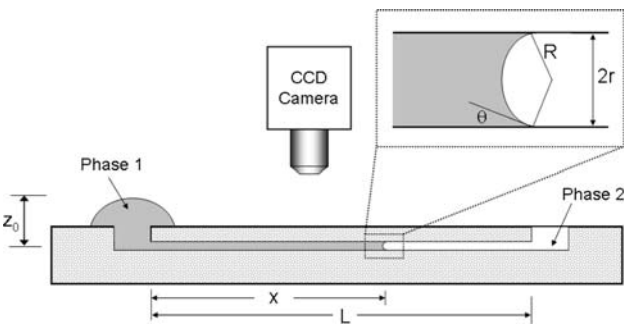

Fig. 1 Two-phase flow in a microchannel with length L and size $2r$ and a geometric representation of the curved interface with a wetting angle θ, and a principal curvature R

and a_0 can be approximated as $\frac{64}{\pi^4}\{1 - \frac{2h}{\pi w}\tanh\frac{\pi w}{2h}\}$. In this case, r in Eq. 2 should be replaced by h. For microfluidic devices, the cross sections of the microchannels are close to either rectangular (e.g., polymer chips) or semi-spherical (e.g., etched glass chips). For the current polymer chips, the aspect ratio of the cross section i.e., $h/w = 0.5$; a_0 therefore has an approximate value of 0.45. For channels with a square cross section, $a_0 = 0.273$.

If the effect of the second phase can be ignored such as that in air–water systems, then Eq. 2 becomes the Washburn equation (Washburn 1921). If the pressure drop ΔP is much smaller than the capillary pressure and the gas phase effect can be ignored, then Eq. 2 can be rewritten as

$$u = a_0\frac{r^2}{8\mu}\frac{P_c}{x}. \tag{4}$$

Equation 4 can be integrated to give an expression of x as a function of time t, i.e.

$$x^2 = a_0\frac{r^2 P_c}{8\mu}t. \tag{5}$$

Assuming that the fluid system is in static equilibrium, the capillary pressure at an interface in a rectangular channel is given by (e.g., Junker et al. 2002)

$$P_c = \sigma\left(\frac{\cos\theta_1 + \cos\theta_2}{w} + \frac{\cos\theta_3 + \cos\theta_4}{h}\right), \tag{6}$$

where σ is the interfacial tension between the two phases; θ_1 and θ_2 are contact angles for the left and right side walls, while θ_3 and θ_4 are contact angles for the top and bottom walls, respectively. For a circular channel with a radius of r, this equation is simplified as

$$P_c = \frac{2\sigma}{r}\cos\theta. \tag{7}$$

3 Experimental details

All the experiments were carried out in the Microfluidics Laboratory in the CSIRO Division of Materials Science and Engineering at Highett, Melbourne, VIC 3190, Australia. The capillary flows were measured in several microfluidic chips and glass capillaries. The details of these microchannels are given below.

3.1 Glass microchannels

The borosilicate square glass capillaries with an inner cross section of 50 × 50 and 500 × 500 μm were purchased form VitroCom (New Jersey, USA). A circular glass capillary with an internal diameter of 50 μm SGE Analytical Science Pty Ltd (Melbourne, VIC, Australia) was also used in the study. The glass chip was purchased from Mycralyne, Edmonton, Canada. The channel layout and the cross section of the channel are shown in Fig. 2. Prior to each experiment the glass chip was cleaned using NaOH (1 mM) solutions and deionised water (DI) and then dried using nitrogen gas. Glass capillaries were used without pretreatment. All the glass microchannels were used without plasma treatment.

3.2 PDMS and PC microchannels

The PDMS and PC microchannels were used in the present investigations. The PDMS chips contained only one straight channel with a rectangular cross section. Two channel sizes were used, one with a cross section of 110 × 220 μm ($h \times w$), and the other of 35 × 70 μm. The PDMS chips were prototyped in the CSIRO Microfluidics Laboratory at Highett, VIC 3190, using a standard photolithography technique. After the PDMS replica (3-mm thickness) was peeled from the mold, holes of 1.5-mm diameter were punched as access ports. The PDMS channels and the capping layer (PDMS) were placed inside the air plasma machine (Harrick PlasmaFlow) for 5-min treatment and then pressed together for bonding. The plasma machine was operated at a frequency of 8–12 MHz with a flow rate of five SCFH (standard cubic feet per hour) and at a pressure of 500 mTorr.

The PC chips were fabricated in the Microfabrication Laboratory in CSIRO Division of Materials Science and Engineering, Clayton, VIC 3169, Australia. The PC chip layout was the same as that shown in Fig. 2, and the channels had a cross section of 35 × 70 μm. Such a layout is mostly used for molecule separation by capillary electrophoresis method. In this study, only the long separation channel was used in investigation. The microfluidic

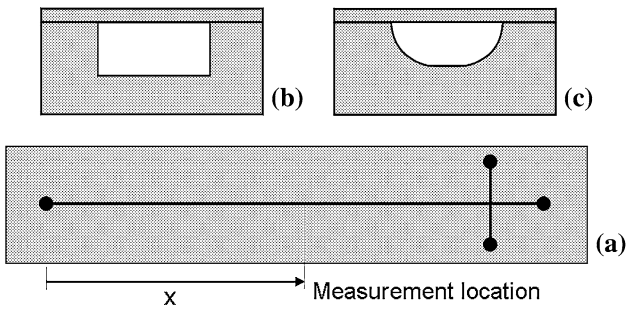

Fig. 2 Microfluidic chip layout and cross sections. The PC chip and the Mycralyne glass chip have the same layout (**a**) while the PDMS chips only have a straight channel. Both the PC and PDMS chips have a rectangular cross section (**b**). The cross section for the glass chip is shown in (**c**). The measurement location x was measured from the inlet port. The glass and polycarbonate chips were originally used for capillary electrophoresis. For these studies, only the long channels were used for measurements

channel pattern was designed using a commercial layout tool and fabricated as a film mask. The mask pattern was exposed into a 35-μm layer of Laminar 5083 resist/stainless steel plate using a collimated UV exposure system. After developing the photoresist, the resulting profile was replicated as a nickel shim by electroplating method. The nickel shim was subsequently used as a die to hot emboss the pattern of channels into polycarbonate chips (16 × 95 mm × 2 mm thick). The access holes were then drilled through the backside of the polycarbonate plate. The finished PC microchannels were then treated with air plasma. The treatment varied from 5 min to 6 h. A 20-μm Mylar film was then laminated as a capping layer to form a sealed channel. The Mylar film was not treated by the plasma. We found that, if treated with plasma, the Mylar film could not be satisfactorily bonded to a PC chip by the laminating process.

For all plasma treatments, the chip components were placed inside the plasma chamber. The channel walls were all uniformly treated. After capping, the four channel walls of the PDMS chips were treated whereas for the PC chips, only three channel walls were treated. The capillary flow was studied for PC chips with and without channel wall preconditioning. For preconditioning, the channels were flushed by a sodium hydroxide (NaOH) solution (1 mM) for 10 min, followed by 10 min of rinsing with DI water and then drying using nitrogen gas.

The measurements of the capillary flow were repeated several times since the first treatment of the channel wall. The capillary flows were monitored over a period of 12 h for the PDMS chip and over 1 month for the PC chip. Table 1 lists all chip dimensions and conditioning parameters.

3.3 Measurement details

In order to study the capillary flow dependence on surfaces, a drop of DI water (~50 μl) was placed in the inlet port and the air–water interface movement was measured by a photographic technique. The objective lenses with a magnification from 4× to 20× were used for different microchannel sizes to measure the interface shape and contact angle as well as monitoring the interface movement for sufficient distance to reliably estimate the speed. Even though the velocity of the interface movement varies with time or distance from the entrance, as indicated by Eqs. 4 and 5, measurements were only taken at one location, i.e., x from the inlet port, for simplicity. The interface movement was imaged over a short distance from x, the maximum distance being around 2 mm. The images of the interface were processed to determine the location of the center of the meniscus (refer to Fig. 2) from x. The resulting drop diameter D was around 4 mm. The corresponding Bond number, i.e., $\frac{\rho g z_0 w}{\sigma}$ (where ρ is the liquid density, σ is the surface tension, g is the gravitational acceleration, z_0 is the liquid height at the inlet, and w is the microchannel cross section length scale) was estimated to be around 0.03. Because the Bond number is much smaller than 1, the effect of drop size and z_0 on capillary flow could be neglected. Further, the curvature of the sample drop was at least two orders of magnitude smaller than that of the interface inside the channel. Therefore, the effect of the Laplace pressure at the entrance port on the interface speed is negligible. This assumption was validated by the experimental observation that the capillary flow almost stopped completely as soon as the interface reached the outlet port.

4 Results

4.1 Glass microchannels

The locations of the air–water interface as a function of time for the glass capillaries and chip are shown in Figs. 3 and 4, respectively. Also shown in the figures are the sample images of the interfaces. The liquid (left-hand side of the interface) had a concave interface with air, which is consistent with the observations of Kim and Whitesides (1997) and Jeong et al. (2007). Although Eq. 5 shows that x is a function of $\sqrt{t}$, the variation with time can be assumed to be linear within a short distance. A least-square fit was applied to the data to quantify the slopes of lines, i.e., the

Table 1 Summary of microchannel and conditioning parameters for capillary flow measurements

Microchip/capillary	Dimensions (μm)	Cross section	Preconditioning	Plasma treatment
Glass capillary	50 × 50	Square	No	No
Glass capillary	500 × 500	Square	No	No
Glass capillary	50	Circular	No	No
Glass chip	50 × 50	Square	Yes, before each test	No
PDMS Chip1	110 × 220	Rectangular	No	5 min at 12 MHz
PDMS Chip2	35 × 70	Rectangular	No	5 min at 12 MHz
PC Chip	35 × 70	Rectangular	Yes, before each test	From 5 min to 6 h at 10 MHz

velocity of the interface movement and the fitted lines are also shown in the figure. These velocities were 2.5, 21.2, and 5.2 mm/s for the circular, large square, and small square capillaries, respectively, at $x = 55$ mm. For all the linear regressions, the coefficient of determination R^2 was in the range of 0.996–0.999.

From the measured velocities, the dynamic contact angles can be calculated using Eq. 4. The calculated contact angles were 72, 76.4, and 54.9° for the circular, large square, and small square capillaries, respectively. The images in Fig. 3 also allowed the dynamic contact angles to be determined for the three capillaries. These values were approximately 65.2, 82.5, and 52.5° (uncertainty ±5°) for the circular, large square, and small square capillaries, respectively. These values agreed reasonably well (±16%) with the calculated values. Regardless of the discrepancies between the measured and calculated values, these contact angles are significantly larger than those measured from a flat glass substrate, i.e., the static contact angles. The latter values are in the range of 0–30°. The large difference between the static and dynamic contact angles is not surprising since at low wetting rate, the dynamic contact angle increases rapidly with the increasing wetting speed (Myers 1999). This fact is also corroborated by the data from Lin and Burns (2005), where the measured meniscus location of the treated COC (cyclic olefin copolymer) microchannels gave a contact of angle of 80° derived from Eqs. 5 and 6. This value is significantly different from the measured value of 45° on the treated COC film. If the value of 45° was used for the contact angle, then the calculated flow speed is twice the measured value. This fact explains why large discrepancies were found between the measured and the calculated flow rates in Jeong et al. (2007) since only

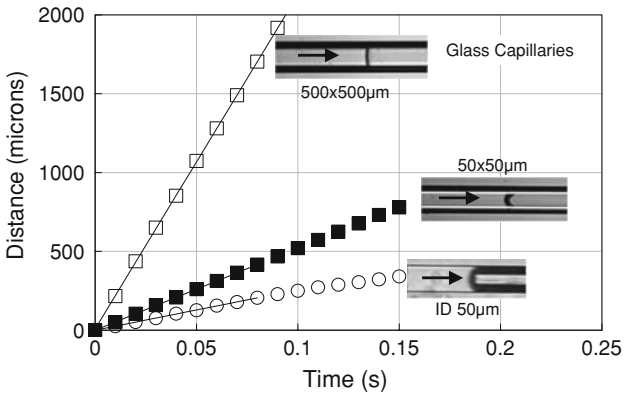

Fig. 3 Interface locations as a function of time for the glass capillaries. Measurement location $x = 55$ mm. The *arrow* indicates the flow direction. The *left-hand side* of the interface is the liquid phase. *Open square* large square capillary tube with 500 × 500 μm cross section, *filled square* small square capillary tube with 50 × 50 μm cross section, and *open circle* circular capillary tube with ID of 50 μm

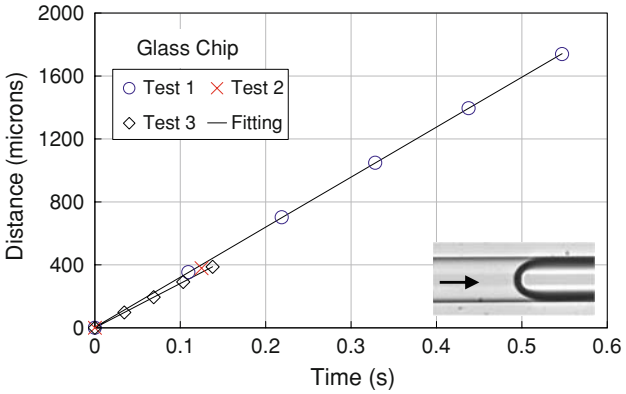

Fig. 4 Interface locations as a function of time for the glass chip. Measurement location $x = 55$ mm. The *arrow* indicates the flow direction. The *left-hand side* of the interface is the liquid phase. The three *symbols* indicate the three tests over an 11-day period

static contact angles were measured and used in the calculation. The present measurement also revealed that the contact angle of the large square channel was larger than that of the small channel even though these were made from the same material and used the same manufacturing process. These findings revealed that, in the calculation of capillary flow speed, dynamic contact angle must be used. Unfortunately, the latter information is not available in most of the previously published studies, since it is more difficult to measure than the static contact angle.

For the glass chip (Fig. 3), three measurements of the capillary flow were carried out during the 2-week period, and all data were reasonably consistent with each other, implying little change was observed among the microchannel surfaces, provided the chip was cleaned using the same methods. The capillary flow velocity was found to be about 3.0 mm/s (to within ±6%). The shape of the cross section is non-standard, and the velocity cannot be calculated using Eq. 4.

4.2 PC and PDMS microchannels

4.2.1 PC

In the case of PC microchips, a low power or a short period of plasma treatment was not significant and could not induce capillary flow. Significant capillary flows could be induced only after the channels were treated for more than 3 h at medium power. Figure 5 shows the interface location as a function of time for one of the PC microchips over a period of 1 month after the air plasma treatment at medium radio frequency (RF) power. A linear regression was also applied to all the data for estimation of flow speed ($R^2 = 0.992$–0.999). Within 45 min of treatment, the flow velocity was estimated to be around 1.5 mm/s. Figure 5 also shows a consistent decay of the capillary flow of the

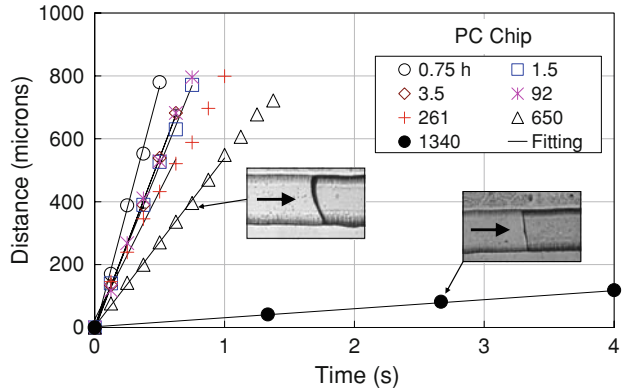

Fig. 5 Interface locations as a function of time since plasma treatment for the PC chip with a cross section of 35 × 70 μm. Measurement location $x = 55$ mm. The *arrow* indicates the flow direction. The *left-hand side* of the interface is the liquid phase

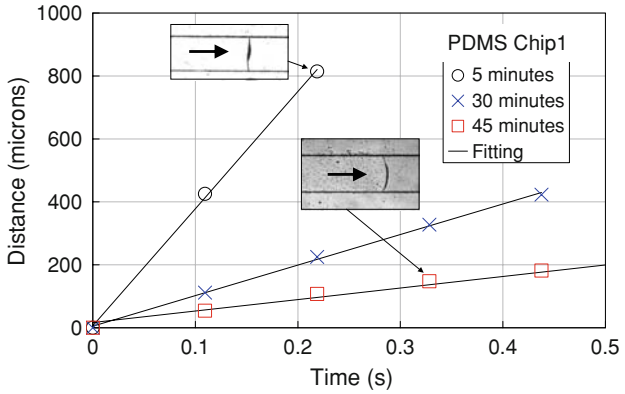

Fig. 6 Interface locations as a function of time since plasma treatment for the PDMS chip with a cross section of 110 × 220 μm. Measurement location $x = 44$ mm. The *arrow* indicates the flow direction. The *left-hand side* of the interface is the liquid phase

chip. However, the capillarity sustained over a month. The sample images of the interface (top inset of Fig. 5) revealed that the shape of the interface meniscus was concave and consistent with that observed from the glass chip. This observation was also consistent with those reported for the square glass tube (Dong and Chatzis 1995) and PDMS microchannels (Kim and Whitesides 1997). Owing to the irregularities of the roughness of both side walls from the hot embossing process, the meniscus was not symmetrical sometimes, and the asymmetry alternated during the movement of the interface. After a long period of time since the treatment, the surface capillarity decayed, and the interface shapes became flatter, as shown in the bottom inset of Fig. 5. The average dynamic contact angle of the channel walls was estimated again from Eq. 4, which value varies from 78° (45 min after treatment) to 88° (native PC surface) after a month.

4.2.2 PDMS

The interface locations as a function of time are shown in Fig. 6 for the PDMS chip with a cross section of 110 × 220 μm (hereafter referred to as PDMS Chip1) and Fig. 7 for the PDMS chip with a cross section of 35 × 70 μm (hereafter referred to as PDMS Chip2). Also shown in the figures are the corresponding linear fittings ($R^2 = 0.997$–0.999). Both figures reveal that the surface property of the PDMS chips could be easily modified in comparison with the PC chip since 5 min of treatment could induce strong capillary flow. At such a short treatment time, the flow speeds were estimated to be approximately 4.0 and 9.1 mm/s for PDMS Chip1 and Chip2, respectively. However, the capillarity decayed quickly over time as indicated by the large changes within 45 min.

The sample images of the meniscus, shown in Figs. 6 and 7 revealed that the shapes of the meniscus were

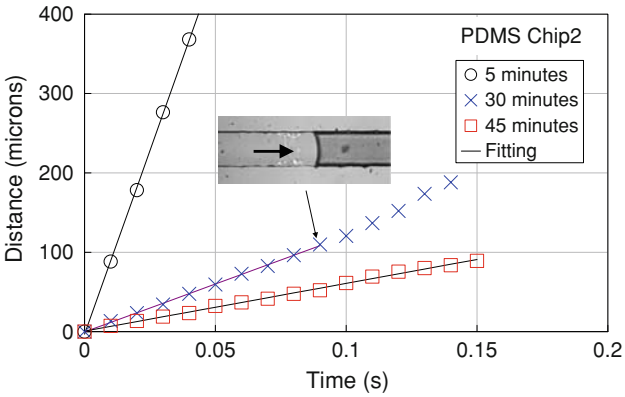

Fig. 7 Interface locations as a function of time since plasma treatment for the PDMS chip with a cross section of 35 × 70 μm. Measurement location $x = 55$ mm. The *arrow* indicates the flow direction. The *left-hand side* of the interface is the liquid phase

different from those observed from the glass and PC channels. A near-flat or convex shape was observed for all the measurements. For example, for the freshly treated PDMS Chip1 (top inset of Fig. 6), the dynamic contact angles for the sidewalls (θ_1 and θ_2) were almost 90°. Subsequently, the interface shape became convex. The dynamic contact angles were measured to be larger than 90° (e.g., $\theta_1 = \theta_2 = 120°$ for the contact angles with sidewalls shown in bottom inset in Fig. 6). If the dynamic contact angles θ_3 and θ_4 were assumed to be the same as θ_1 and θ_2, Eq. 6 implies that the capillary pressure P_c is zero or negative (i.e., lower pressure in the liquid side), and the interface should be stationary or move in the opposite direction. This would contradict with the experimental observations.

The fact that the interface moved with a significant speed even though the meniscus was nearly flat or convex

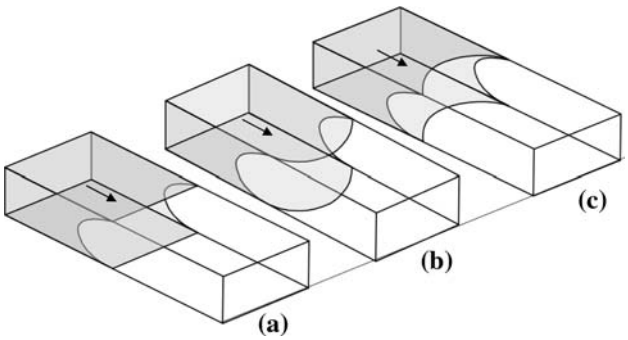

Fig. 8 Schematic summary of different shapes of air–water interfaces in the microchannels. **a** Interface with concave contact lines for side walls and near-flat contact lines for top and bottom walls (PDMS chip shown in the *top insert* of Fig. 6); **b** interface with concave contact lines for side walls and convex contact lines for top and bottom walls (PDMS chip shown in the *bottom insert* of Fig. 6); **c** interface with concave contact lines for all walls (glass and treated PC chips). The *dark areas* represent water phase. All the interfaces move from *left* to *right*

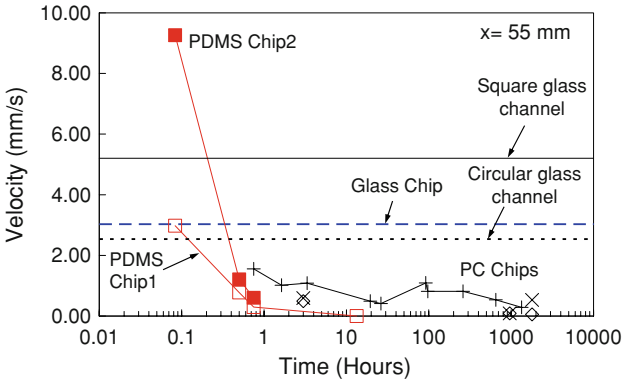

Fig. 9 Variation of the capillary flow velocity for PDMS and PC chips as a function of time since air plasma treatment. $x = 55$ mm. *Solid square* PDMS chip with 100 × 200 μm cross section; *Open square* PDMS chip with 35 × 70 μm cross section; *open diamond*, *times*, *plus* three PC chips of same cross section 35 × 70 μm. The three lines represent velocities for the three glass channels, i.e., (from top to bottom) the square glass tube (50 μm), glass chip, and the circular glass channel, respectively

implies that the actual contact angles of the interface with the top and bottom walls, i.e., θ_3 and θ_4, were smaller than 90°, and the resulting capillary pressure P_c was still positive. Thus, a positive flow could still maintain even though the sidewall contact angles are larger than 90°. This is similar to the flow induced by the glass/PDMS hybrid microchannels (Jeong et al. 2007). Therefore, the three-dimensional interface in the treated PDMS microchannels should be of the shape as depicted in Fig. 8a and b. The latter was also proposed by Zhao et al. (2001). The projection of the interface onto the top and bottom planes shows a convex or near-flat interface, as imaged during experiments. For the glass and PC microchannels or those observed in Dong and Chatzis (1995), Kim and Whitesides (1997), and Jeong et al. (2007), the contact angles were smaller than 90° for all the side walls, and the interface shape is different as shown in Fig. 8c. From Eqs. 4 and 6, the contact angles θ_3 and θ_4 for the three measurements in Fig. 6 were calculated to be 74.5, 79.5, and 79.8, respectively. This indicates that the recovery of the contact angle to the native value was different between the side and top/bottom walls.

4.3 Capillary flow velocity

The velocities of the interface movement estimated using the least-square fit method for all the microchannels are summarized in Fig. 9. All the velocity data were obtained at the same x value of 55 mm except for the data of PMDS Chip1. The latter data were obtained at $x = 44$ mm, and the corresponding velocities at $x = 55$ mm were estimated using $u|_{x=55} = u|_{x=44} * 44/55$ since the velocity is inversely proportional to x according to Eq. 4. These converted values are shown in the figure for simplicity of comparison. The freshly treated PDMS Chip1 showed a similar level of hydrophilicity as that of the glass chip, as indicated by the similar capillary flow velocity of ~3 mm/s. The hydrophilic property of the PDMS chips decreased rapidly, and the hydrophilicity was lost overnight. Figure 9 shows the small PDMS channel (PDMS Chip2) had a much higher capillary flow velocity than that of the large channel. This seemed to be contradictory to the theory since, from Eq. 4, $u \propto r^2$ and larger channels should have a much faster capillary flow. The larger capillary flow of the small PDMS channel was due to the more intensive plasma treatment since a high RF power was used instead of the medium power for the large PDMS channel.

In the case of PC chips, the air plasma treatment could induce significant capillary flow, albeit lower than those in glass chips and freshly treated PDMS chips. However, the capillarity could last for a much longer time. Figure 9 shows that there was an initial drop in the flow rate since the plasma treatment. However, the data showed a systematic but slower decrease over the next few days or so. The capillary flow rate could sustain above approximately 0.5 mm/s. These data were obtained when the chip was used without preconditioning. However, when the chip was cleaned with NaOH solution (1 mM) followed by DI water rinsing and drying, the capillary flow rate was increased to approximately 1.05 mm/s, which was close to that measured only a few hours since treatment. The subsequent measurements over 1 month period showed a steady but slow reduction in the flow rate. The last measurement had a value of 0.55 mm/s.

5 Conclusions

The capillary flows in several glass tubes and fabricated microchannels were studied experimentally. The effect of plasma treatment on the capillarity of microfluidic chips was also investigated. The capillary flow was measured using a photographic technique and image processing. The glass chip or capillaries were used without treatment while the PC and PDMS chips were treated using air plasma.

The capillary flows in the glass capillaries showed that the dynamic contact angles were significantly larger than the static contact angles measured from a flat glass substrate. The dynamic contact angle varied with channel size, as was also observed by Ichikawa et al. 2004. These findings suggest that, in the theoretical calculations of capillary flow speed, dynamic contact angle measured in situ must be used, especially for microfabricated microchannels since the surface properties are likely to be different from the native material.

Even though this study found similar behavior of plasma treatment effect on the capillary flow in PDMS and PC microchannels to those reported previously for different polymer chips, it was revealed from this study that plasma treatment could induce different interface shapes in the PDMS channels from those in the glass and PC channels. The PDMS channel walls could acquire different levels of hydrophilicity during the plasma treatment, and the recovery to hydrophobicity was also non-homogeneous.

Acknowledgment Special thanks go to Drs. P. W. Leech and B. A. Sexton for their contribution for the fabrication of the polycarbonate microfluidic chips.

References

Beebe DJ, Mensing GA, Walker GM (2002) Physics and applications of microfluidics in biology. Annu Rev Biomed Eng 4:261–286

Belder D, Ludwig M (2003) Surface modification of poly(dimethylsoloxane) microchannels. Electrophoresis 24:3595–3606

Bodas D, Rauch JY, Khan-Malek C (2008) Surface modification and aging studies of addition-curing silicone rubbers by oxygen plasma. Eur Polym J 44:2130–2139

Brody JP, Yager P, Goldstein RE, Austin RE (1996) Biotechnology at low Reynolds numbers. Biophys J 71:3430–3441

Chung KH, Hong JW, Lee D, Yoon HC (2007) Microfluidics chip accomplishing self-fluid replacement using capillary force and its bioanalytical application. Anal Chim Acta 585:1–10

Chung S, Yun H, Kamm RD (2009) Nanointerstice-driven microflow. Small 5:609–613

Dong M, Chatzis I (1995) The imbibition and flow of a wetting liquid along the corners of a square capillary tube. J Colloid Interface Sci 172:278–288

Fritz JL, Owen MJ (1995) Hydrophobic recovery of plasma-treated polydimethylsiloxane. J Adhes 54(1–4):33–45

Ichikawa N, Hosokawa K, Maeda R (2004) Interface motion of capillary-driven flow in rectilinear microchannel. J Colloid Interface Sci 280:155–164

Jeong HE, Kim P, Kwak MK, Seo SH, Suh KY (2007) Capillary kinetics of water in homogenous hydrophilic polymeric micro- to nanochannels. Small 3(5):778–782

Junker D, Schmid H, Dreschsler U, Wolf H, Michel B, Rooij N, Delamarche E (2002) In: Proceedings of MicroTAS 2002 conference, Nara, Japan, vol 2, pp 952–954

Kim E, Whitesides GM (1997) Imbibition and flow of wetting liquids in noncircular capillaries. J Phys Chem 101:855–863

Kim E, Xia Y, Whitesides GM (1995) Polymer microstructures formed by moulding in capillaries. Nature 376:581–584

Kim J, Chaudhury MK, Owen MJ, Orbeck T (2001) The mechanism of hydrophobic recovery of polydimethylsiloxane elastomers exposed to partial electrical discharges. J Colloid Interface Sci 244:200–207

Kirby BJ, Hasselbrink J, Ernest F (2004) Zeta potential of microfluidics substrates: 2. Data for polymers. Electrophoresis 25:203–213

Klages C-P, Berger C, Eichler M, Thomas M (2007) Microplasma-based treatment of inner surface in microfluidics devices. Contrib Plasma Phys 47:49–56

Landau LD, Lifshitz EM (1987) Fluid mechanics, 2nd edn. Pergamon Press, Oxford

Lim H, Lee Y, Cho HY, Kim KJ (2001) Surface treatment and characterization of PMMA, PHEMA A and PHPMA. J Vac Sci Technol A 19(4):1490–1496

Lim YT, Kim S-J, Yang H, Kim K (2006) Controlling the hydrophilicity of microchannels with bonding adhesives containing surfactants. J Micromech Microeng 16:N9–N16

Lin R, Burns MA (2005) Surface-modified polyolefin microfluidic devices for liquid handling. J Micromech Microeng 15:2156–2162

Martin IT, Dressen B, Boggs M, Liu Y, Fisher ER (2007) Plasma modification of PDMS microfluidic devices for control of electroosmotic flow. Plasma Process Polym 4:414–424

Moon MW, Vaziri A (2009) Surface modification of polymers using a multi-step plasma treatment. Scr Mater 60:44–47

Myers D (1999) Surfaces, interfaces, and colloids: principles and applications, 2nd edn. Wiley–VCH, New York

Squires TM, Quake SR (2005) Microfluidics: fluid physics at the nanoliter scale. Rev Mod Phys 77:977–1026

Vourdas N, Tserepi A, Boudouvis AG, Gogolides E (2008) Plasma processing for polymeric microfluidics fabrication and surface modification: effect of super-hydrophobic walls on electroosmotic flow. Microelectron Eng 85:1124–1127

Washburn EW (1921) The dynamics of capillary flow. Phys Rev 17:273–283

Whitesides GW (2006) The origins and the future of microfluidics. Nature 442:368–373

Zhao B, Moore JS, Beebe DJ (2001) Surface-driven liquid flow inside microchannels. Science 291:1023–1026